

THERMAL BEHAVIOUR AND VIBRATIONAL CHARACTERIZATION OF $MH_2(IO_3)_3$ PHASES ($M = K, Rb$ and NH_4)

M. B. Vassallo and I. L. Botto

QUIMICA INORGANICA, FACULTAD DE CIENCIAS EXACTAS, UNIVERSIDAD NACIONAL DE LA PLATA, LA PLATA 1900, ARGENTINA

The thermal behaviour of the $MH_2(IO_3)_3$ ($M = K, Rb$ and NH_4) isomorphous compounds, as well as the IR and Raman spectra have been investigated as part of a study of the properties of solid protonic conductors. Detailed stoichiometries, sustained by TG, DTA, XRD and IR analysis, have been developed into the three phases. There were also evidences of the formation of the $[I_3O_8]^-$ polymeric phases. Their stabilities were associated to the different polarizing power of the H, K and Rb cations.

Keywords: isomorphous compounds, solid protonic conductors, TG, DTA, XRD, IR

Introduction

The solid protonic conductors, which are materials used for electrode and fuel cells, have lately led to a lot of investigations. The structural, thermal and spectroscopic characterization of these phases are undoubtedly related to the protonic mobility.

The ammonium diacid iodate $(NH_4)H_2(IO_3)_3$ has been found to exhibit protonic conductivity [1]. Although the literature provides general information about the $MH_2(IO_3)_3$ phases ($M = K, Rb$ and NH_4) this is not clear enough [2-9] and the crystal structure of the ammonium and potassium isomorphous salts have been recently analyzed and compared [10]. The present inform attempts to clarify some aspects of these systems. Thus, the thermal and vibrational behaviour of this series have been reported.

Experimental

The monovalent (ammonium, potassium and rubidium) diacid iodates were obtained by evaporating aqueous solution of I_2O_5 and respective $MHCO_3$ in dilute sulfuric acid. Small crystals were used as seeds to obtain large crystals by evaporating the solutions.

Powder diffraction data were obtained with a Philips PW 1730 diffractometer, using $CuK\alpha$ radiation (nickel filter).

IR spectra were recorded with a Perkin Elmer 580-B Spectrophotometer using the CsCl-pellet as well as the nujol technique.

Raman spectra were obtained with a Spex-Ramalog 1403 double monochromator spectrometer, equipped with a SCAMP data processor. The 514.5 nm line of an Ar-ion laser was used for exciting the samples.

The TG and DTA thermal analysis were carried out using a Rigaku CN 8002 L2 thermoanalyzer. The measurements were performed under a N_2 stream ($0.4 \text{ l}\cdot\text{min}^{-1}$). The temperature was raised up to 700°C (heating rate $10 \text{ deg}\cdot\text{min}^{-1}$). The specimens were analyzed against $\alpha\text{-Al}_2\text{O}_3$ as reference. Additional thermal studies were carried out in a crucible furnace. The samples were investigated by X-ray diffractometry and IR spectroscopy.

Results and discussion

According to the X-ray and neutron diffraction studies, the potassium, rubidium and ammonium diacid iodates are isomorphous phases. They belong to the triclinic system, space group $P1$ and $Z = 2$. More recent cell parameters data are shown in Table 1. Although the literature data are not entirely consistent [10], these lattices are structurally built up by a framework of strongly distorted IO_6 octahedra (three I-O bonds are close to 1.8 \AA while the other three are farther away at 2.7 \AA) [7, 10]. The polyhedra are linked together by corner sharing and by H-bonds in the ammonium compounds. On the other hand, there are I-O...(H) and I-O...(M) bonds in the remaining K- and Rb-isomorphous phases. The NH_4 and K cations should be considered in a ten coordination [10]. On the other hand, there are three types of slightly different IO_6 polyhedra in the lattice with one common corner and a very complex and highly condensed structural group. Two of these groups are linked in a block of six octahedra, repeated along the three crystallographic axis. This type of framework generates cavities (occupied by the M ions) and also channels running along the three axis of the triclinic lattice, in which the acids protons are located [10]. These H-atoms can easily be removed when an electric field is applied and their migration is responsible for the ionic conductivity. The transversal dimensions of the channels are shorter in $KH_2(IO_3)_3$ than in the ammonium compound. So, the movement of the protons in-

side the channels is lower in the K phase. Likewise, as the ammonium ion is not very different in size from the Rb ion [11], the XRD patterns for both compounds are similar. Only a very slight shift of the diffraction lines to smaller angles is observed in the last compound.

Table 1 Cell parameters of $MH_2(IO_3)_3$ ($M = K, NH_4, Rb$)

| | $KH_2(IO_3)_3$ [10] | $NH_4H_2(IO_3)_3$ [10] | $RbH_2(IO_3)_3$ [7] |
|--------------|---------------------|------------------------|---------------------|
| a (Å) | 8.266 | 8.396 | 8.332 |
| b (Å) | 8.200 | 8.363 | 8.232 |
| c (Å) | 8.180 | 8.207 | 8.264 |
| α (°) | 66.08 | 65.57 | 60.66 |
| β (°) | 60.16 | 60.13 | 85.80 |
| γ (°) | 71.06 | 70.33 | 66.10 |

Finally, comparing the ammonium and potassium structural information, it is possible to get the following conclusions:

- i) In the framework, there are three shorter I–O distances.
- ii) The I–O...(K) bond-length is increased in relation to the I–O...(NH₄) one.
- iii) The shortening of the I–O...(H_{prot}) bond is more evident in the case of the K phase. Therefore, a lengthening of the O–H_{prot} distance is observed in this case.
- (iv) Finally, the shortest H_{prot}–H_{prot} distance (into the channels) is observed in the K phase.

Vibrational behaviour

The IR and Raman spectra of the ammonium and potassium compounds were recently published by Santha *et al.* [12]. However, whereas the Raman lines agree with our results, the IR spectra show differences. This discrepancy is attributed to the fact that the samples were prepared using the KBr pellet technique. As it is known, under these conditions an immediate redox reaction, between the iodate acid and the Br⁻ ions takes place, which alters the original composition of the sample. This observation has been experimented in our laboratory and for this reason the vibrational behaviour of all members of the series has been analyzed in CsCl as well as in nujol [13, 14].

Figure 1 shows a typical vibrational spectrum of the (NH₄)H₂(IO₃)₃ phase, registered between 1300–200 cm⁻¹. Four fundamental vibrational frequencies, all IR and Raman active, are to be expected for IO₃(C_{3v}) pyramidal symmetry: ν_1 (symmetric stretching) at 780 cm⁻¹, ν_2 (symmetric bending) at 390 cm⁻¹, ν_3 (antisymmetric stretching) at 830 cm⁻¹ and the ν_4 (antisymmetric bending) at 330 cm⁻¹ [15, 16]. Likewise, it is usual that the 2 ν_2 symmetric bending overtone,

appears in the Raman effect in the stretching region ($700\text{--}800\text{ cm}^{-1}$) and its intensity can be amplified by Fermi resonance with the ν_1 symmetric mode. Thus it is difficult to assign the spectra correctly because, although the strongest IR bands can be attributed to the ν_3 components, it is not so clear to distinguish between $2\nu_2$ and ν_1 modes in the Raman effect [17].

On the other hand, the I-O-H vibrations are usually observed in the $1300\text{--}1100\text{ cm}^{-1}$ region (δ I-O-H), as well as near 650 cm^{-1} (ν I-O-(H)) [18]. In the first region, the δ I-O-H vibration is splitted and located at higher frequencies than those observed for the free iodic acid [19]. This can be explained by the increase of the I-O-H angle, similar to that found in $\text{BeH}_2(\text{IO}_3)_3 \cdot 6\text{H}_2\text{O}$ [20].

Table 2 gives the frequencies of the vibrational spectra of the $\text{MH}_2(\text{IO}_3)_3$ ($M = \text{K}, \text{Rb}$ and NH_4) phases. The assignment has been done on the basis of very distorted and condensed IO_3 groups. It is clear that the ammonium and rubidium

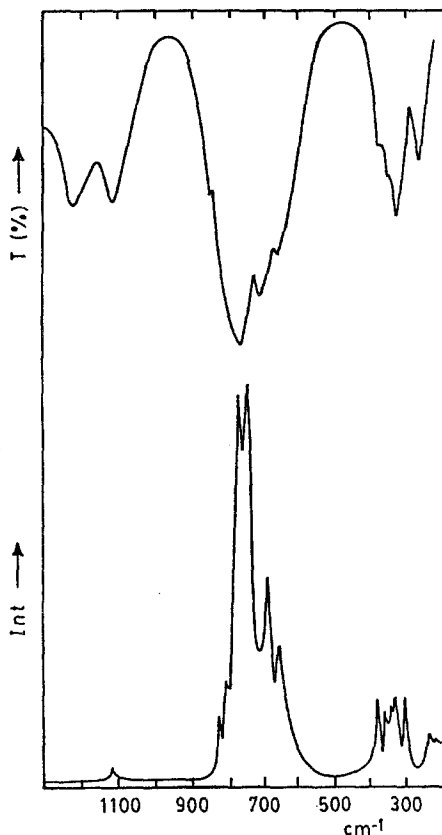


Fig. 1 Vibrational spectrum of $(\text{NH}_4)\text{H}_2(\text{IO}_3)_3$ (between $1300\text{--}200\text{ cm}^{-1}$) Top: IR; bottom: Raman

spectra show similar and comparable values, fundamentally for the I-O...M stretching modes, but they are located at higher frequencies than the corresponding to the $\text{KH}_2(\text{IO}_3)_3$ spectrum.

Thermal behaviour

The TG and DTA traces recorded in typical experiments for $\text{MH}_2(\text{IO}_3)_3$ ($M = \text{K, Rb, NH}_4$) are shown in Fig. 2. It is evident that the thermal behaviour for the NH_4 -compound differs from the remaining isomorphous phases.

Table 2 Vibrational behaviour of $\text{MH}_2(\text{IO}_3)_3$ ($M = \text{K, NH}_4, \text{Rb}$). Values in cm^{-1}

| $\text{KH}_2(\text{IO}_3)_3$ | | $\text{NH}_4\text{H}_2(\text{IO}_3)_3$ | | $\text{RbH}_2(\text{IO}_3)_3$ | | Assign. |
|------------------------------|--------|--|---------|-------------------------------|--------|------------------------|
| IR | Raman | IR | Raman | IR | Raman | |
| | | 3220 br | 3200 w | | | ν N-H |
| | | 1430 m | 1430 vw | | | ν N-H |
| 1230 w | | 1220 m | | 1220 m | | δ I-O-H |
| 1090 w | | 1110 w | 1115 vw | 1085 w | | |
| 825 sh | 822 w | 843 sh | 823 w | 843 sh | 828 w | ν_3 IO_3 |
| 790 s | 801 w | 790 sh? | 804 w | 790 sh | 800 w | |
| 755 s | 759 s | 765 vs | 762 vs | 762 vs | 764 vs | ν_1 IO_3 |
| | 741 vs | | 747 vs | | 748 vs | $2\nu_2$ IO_3 |
| 710 sh | 685 m | 710 m | 687 m | 710 m | 689 m | ν I-O...(H) |
| 625 m | 654 m | 665 m | 660 sh | 640 m | 662 m | |
| 385 sh | 372 w | 375 sh | 373 w | 380 sh | 374 w | ν_2 IO_3 |
| | 352 w | 360 sh | 352 w | 360 sh | 350 w | |
| 340 m | 339 w | 335 m | 338 w | 340 m | 339 w | ν_4 IO_3 |
| | 330 w | | 328 w | | 328 w | |
| 310 m | | | | | | lattice modes |
| | 302 w | | 301 w | | 302 w | |
| 285 sh | | 290 m | | 295 w | | |
| | 234 vw | | 233 vw | | 234 vw | |
| | 215 vw | | 213 vw | | 212 vw | |

s: strong; vs: very strong; m: medium; w: weak; vw: very weak; sh: shoulder; br: broad

a) $\text{NH}_4\text{H}_2(\text{IO}_3)_3$

As it is observed in Fig. 2c, the DTA curve of this phase shows a small exothermic peak at 200°C and two well developed endothermic peaks at 158° and 420°C respectively. They are identified with two strong weight-losses on the TG curve, one located between 155° – 200°C and the other between 390° – 420°C . In the first one, there seems to be two successive and partially superposed processes of difficult resolution. The formation of the $\text{NH}_4\text{IO}_3\text{I}_2\text{O}_5$ phase, suggested in

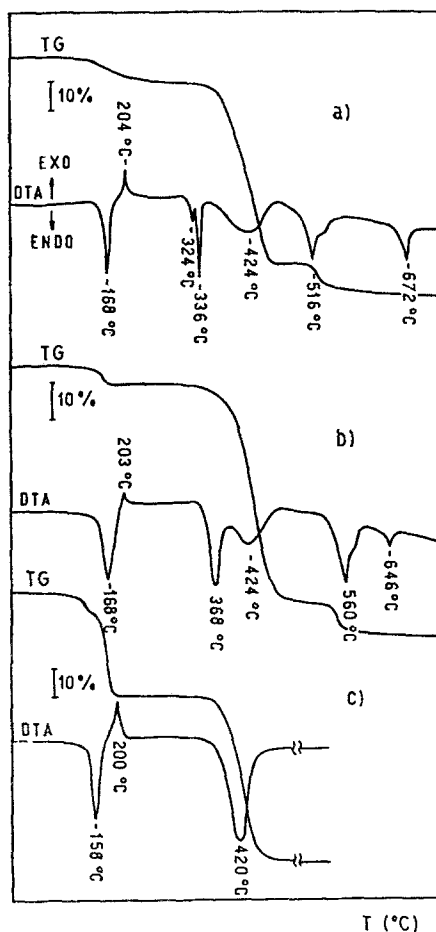
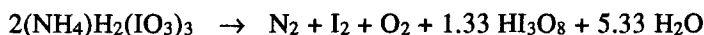


Fig. 2 TG and DTA plots of: a) $\text{KH}_2(\text{IO}_3)_3$, b) $\text{RbH}_2(\text{IO}_3)_3$, c) $\text{NH}_4\text{H}_2(\text{IO}_3)_3$

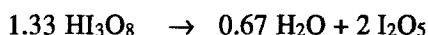
the literature [21] has not been detected and iodine is given up at $\approx 160^\circ\text{C}$. Likewise, IR spectra of samples heated at this temperature have not shown the typical N-H vibrations. On the other hand, the spectra of the polymeric HI_3O_8 species [19, 22] have been clearly observed near 200°C , as an intermediate phase which easily becomes I_2O_5 . The presence of HI_3O_8 depends fundamentally on the heating rate and on the particle size of the sample. The small exothermic peak is associated with this formation. The second step of the thermal treatment (420°C) corresponds to the I_2O_5 decomposition with the evolution of I_2 and O_2 [23] with a 100% weight loss. Hence, from the experimental weight-loss values, 38.5% for the first overall process and 61.5% for the second one, and with the aid of the IR

spectroscopy and XRD techniques, the degradation process can be formulated as follows:

First step: (158°–204°C):

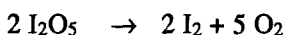


(partial weight loss: 37.6%)



(partial weight loss: 0.9%)

Second step (420°C):



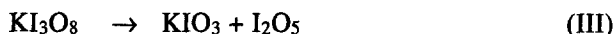
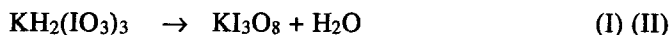
This behaviour resembles the thermal $\text{NH}_4\text{H}(\text{IO}_3)_2$ compound [24].

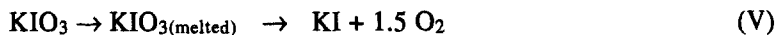
b) $\text{MH}_2(\text{IO}_3)_3$ ($M = \text{K}, \text{Rb}$)

As it can be observed in Fig. 2a and b, the DTA curves of both compounds show a greater number of thermal effects in relation to the ammonium phase.

The first endothermic peaks in both compounds are attributed to the dehydration process with the subsequent rearrangement of the lattice for the formation of the polymeric MI_3O_8 crystalline phase. This can be clearly identified by starting from 210°C, and its formation is surely associated to the small exothermic peak. These polymeric phases are related to HI_3O_8 but this last species is more unstable [23]. Figure 3 shows a comparison of the KI_3O_8 , RbI_3O_8 and HI_3O_8 IR spectra, which are all intermediate phases. The characteristic stretching of the I–O–I bridges are observed in the 400–650 cm^{-1} . The stretchings and bendings of the iodate groups [19] are located between 650–850 and below 400 cm^{-1} respectively. The stability of the MI_3O_8 remains up to 350°C approximately, and for the cation with the more polarizing power, the stability is lower. So, the decomposition process occurs at 338° and 360°C for the K and Rb compounds respectively.

The subsequent formation of the respective MIO_3 and I_2O_5 is clearly observed, without weight loss, at these temperatures, in agreement with the endothermic peaks. Table 2 shows the different steps of the $\text{KH}_2(\text{IO}_3)_3$ and $\text{RbH}_2(\text{IO}_3)_3$ thermal process which can be sustained with the aid of the XRD and IR spectroscopy. The complete and typical decomposition scheme for the potassium phase is the following:





Conclusions

In a first place, it is important to remark that the KBr pellet technique for the IR measurements cannot be used in these systems, due to the redox reaction between the bromide and iodate acid species, situation that induces to erroneous results. For this reason, the IR previous data [12] are not reliable.

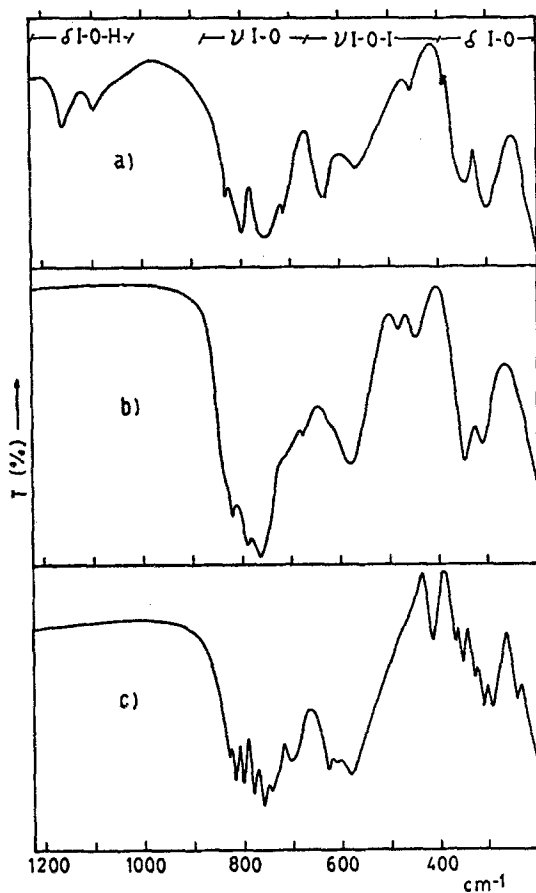


Fig. 3 IR spectra of the intermediate phases of the thermal process: a: HI_3O_8 , b: KI_3O_8 , c: RbI_3O_8

Table 3 $\text{KH}_2(\text{IO}_3)_3$ and $\text{RbH}_2(\text{IO}_3)_3$ thermal process

| Type of reaction | $\text{KH}_2(\text{IO}_3)_3$ | | | | | | | $\text{NH}_4\text{H}_2(\text{IO}_3)_3$ | | | | | |
|---------------------------|------------------------------|-----|-----|-----|-------|------|-----|--|-----|-----|-------|------|-----|
| | EN | EX | EN | EN | EN | EN | EN | EN | EX | EN | EN | EN | EN |
| $T / ^\circ\text{C}$ | 168 | 204 | 324 | 336 | 424 | 516 | 672 | 168 | 203 | 368 | 424 | 560 | 646 |
| theor. weight loss / % | 3.18 | — | — | — | 59.00 | 8.48 | — | 2.94 | — | — | 54.53 | 7.84 | — |
| exp. weight loss / % | 3.20 | — | — | — | 59.10 | 8.47 | — | 2.96 | — | — | 54.52 | 7.86 | — |
| step | I | II | III | III | IV | V | VI | I | II | III | IV | V | VI |

EN: endothermic, EX: exothermic

From the XRD and vibrational appreciation, the $\text{RbH}_2(\text{IO}_3)_3$ cell dimensions as well as the I–O distances are expected to be comparable to the ammonium compound. Then a good protonic mobility can also be predicted for the Rb-phase.

On the other hand, the thermal treatment of the NH_4^- as well as K- and Rb-phases does not occur in a similar way; however, the presence of the $[\text{I}_3\text{O}_8]^-$ polymeric and unstable species can be observed, as an intermediate phase, in all compounds, previous to the I_2O_5 formation. Likewise, the thermal behaviour of the MI_3O_8 ($M = \text{K}, \text{Rb}$) is affected by the polarizing power of the cation. These polymeric phases are easily characterized by IR spectroscopy, presenting typical I–O–I vibrations between $400\text{--}600\text{ cm}^{-1}$, besides the correspondent to the I–O stretching and bending.

* * *

This work was supported by CONICET (Programa QUINOR) and CICPBA.

References

- 1 A. L. Baranov, G. O. Dobrzanski, V. V. Ilyukhin, V. S. Ryabkin, Yu. N. Sokolov, N. I. Sorokina and L. A. Shuvalov, *Krist.*, 26 (1981) 1259.
- 2 F. A. Alton and J. J. O'Connor, *Mater. Res. Bull.*, 6 (1971) 653.
- 3 T. G. Balicheva and G. Petrova, *Prob. Sourem Khim. Koord. Soedin.*, 4 (1974) 266, C. A. 82-147674 z.
- 4 V. I. Vavilin, I. F. Burshtein, B. M. Schchedrin, V. V. Ilyukhin and N. V. Belov, *Dokl. Akad. Nauk. SSSR*, 226 (1976) 1073, C. A. 84-143246 e.
- 5 A. I. Baranov, G. F. Dobrzanski, V. V. Ilyukhin, V. P. Kalinin, V. S. Ryabkin and L. A. Shuvalov, *Krist.* 24 (1979) 280.
- 6 Fu Zhengmin, Li Wenxin and Chen Liquan, *Wuli Xuebao*, 30 (1981) 1383, C. A. 226563 j.
- 7 Fu Zhengmin, Li Wenxin, Dai Jinbi and Liang Dongcai, *Wuli Xue, Xue bav*, 3 (1987) 35, C. A. 106-129711.
- 8 E. A. Soldatov, V. V. Ilyukhin, E. A. Kuzlmin and N. V. Belov, *Dokl. Akad. Nauk. SSSR*, 252 (1980) 615., C. A. 93-123992 e.

- 9 N. I. Sorokina, L. A. Muradyan, A. A. Loshmanov, L. E. Fykin, E. E. Rider, G. F. Dobrzhanskii and V. I. Simonov, *Krist.*, 29 (1984) 220.
- 10 P. Bordet, J. X. Boucherle, A. Santoro and M. Marezio, *Solid State Ionics*, 21 (1986) 243.
- 11 R. D. Shannon, *Acta Crystallogr.*, A32 (1976) 751.
- 12 N. Santha, M. Isaac, V. U. Nayar and G. Keresztury, *J. Raman Spectrosc.*, 22 (1991) 419.
- 13 E. J. Baran and P. J. Aymonino, *Spectrochim. Acta*, 24A (1968) 288.
- 14 E. J. Baran and P. J. Aymonino, *Monatsh. Chem.*, 99 (1968) 606.
- 15 K. Nakamoto, 'Infrared and Raman Spectra of Inorganic and Coordination Compounds', 3rd Ed., J. Wiley, New York 1978.
- 16 H. Siebert, 'Anwendungen der Schwingungsspektroskopie in der anorganischen Chemie' Springer-Verlag, 1966.
- 17 W. E. Dasent and T. C. Waddington, *J. Chem. Soc.*, (1960) 2429.
- 18 M. Maneva and M. Georgiev, *Spectroscopy Lett.*, 23 (1990) 831.
- 19 Th. Dupuis and J. Lecomte, *Comp. Rendus Acad. Sci. Paris*, 252 (1961) 26.
- 20 M. Maneva and M. Georgiev, *Polyhedron*, 8 (1989) 357.
- 21 A. M. Pertosyan and V. B. Gavalyan, *Zh. Neorg. Khim.*, 31 (1986) 2491.
- 22 P. M. A. Sherwood and J. J. Turner, *Spectrochim. Acta*, 26A (1970) 1975.
- 23 K. Selte and A. Kjekshus, *Acta Chem. Scand.*, 22 (1968) 3309.
- 24 C. Duval, 'Inorganic Thermogravimetric Analysis', 2nd Ed., Elsevier, 1963.

Zusammenfassung — Als Teil einer Studie der Eigenschaften von Feststoff-Protonenleitern wurde neben den IR- und Raman-Spektren auch das thermische Verhalten der isomorphen Verbindungen $MH_2(IO_3)_3$ ($M = K, Rb, NH_4$) untersucht. In den drei Phasen wurden mit Hilfe von TG, DTA, IR und Röntgendiffraktionsuntersuchungen detaillierte Stöchiometrien entwickelt. Es gab auch Beweise für die Bildung von polymeren $[I_3O_8]^-$ Phasen. Ihre Stabilität steht in Verbindung mit der unterschiedlichen Polarisationsfähigkeit der H-, K- und Rb-Kationen.